01

Approximation of the electronic term of the diatomic molecule by the Morse function. Inversion of anharmonicity

© G.S. Denisov, I.K. Tokhadze, R.E. Asfin

St. Petersburg State University, St. Petersburg, Russia

e-mail: iktpen1@yandex.ru

Received June 24, 2025
Revised June 24, 2025
Accepted July 25, 2025

The approximation of interatomic potentials in diatomic molecules using the Morse potential typically leads to an overestimated bond energy, calculated as $D'_e = \omega_e^2/4\omega_e x_e$, based on known values of ω_e and $\omega_e x_e$ determined from the first two vibrational transitions, 0−1 and 1−2. This relationship holds true for a wide range of molecules, such as H_2, O_2, N_2, HF, HCl, and many others. However, for some molecules and diatomic ions, the extrapolated value of the bond energy D'_e turns out to be lower than the actual value D_e. In such molecules, the shape of the potential energy curve deviates significantly from the standard form due to a broadening in the lower part of the potential well, which manifests as a large anharmonicity $\omega_e x_e$. This feature is conveniently analyzed using the difference $\delta(r) = U(r) - M(r)$ between the actual potential and its Morse approximation. This type of approximation yields a Morse solution $M1(r)$ that accurately describes the lower part of the potential for the simple molecules, with a monotonic increase in deviation as it approaches the dissociation asymptote. An alternative solution, $M2(r)$, is constructed based on the known values of D_e and ω_e, while the anharmonicity $\omega_e x'_e$ is computed $\omega_e x'_e = \omega_e^2/4D_e$. The $M2(r)$ approximation provides a better description of the upper part of the potential and a satisfactory representation of the lower part. The deviation from the actual potential takes the form of a bell-shaped curve, whose maximum is typically located above the midpoint of the potential well. This paper presents several examples of potentials of a special type, for which $D'_e < D_e$ and $\omega_e x_e > \omega_e x'_e$, a behavior that can be termed the term inversion of anharmonicity.

Keywords: diatomic molecules, Morse potential, anharmonicity, vibrational structure, potential function approximation.

DOI: 10.61011/EOS.2025.09.62302.8313-25

1. Introduction

In [1–5], the properties of the Morse potential function and its specific application for approximating the electronic terms of diatomic molecules were described in detail. A group of simple terms was identified, whose shapes do not differ significantly from the Morse contour. For this group, systematic approximation errors were characterized, and a method for their analysis was presented. Morse succeeded in constructing a simple anharmonic potential that approximates real terms $U(r)$ quite well. Its important feature is the existence of two variants of approximation $M1(r)$ and $M2(r)$.

In the original work [6], Morse proposed a potential of the form

$$U(r) = D_e[1 - e^{-a(r-r_e)}]^2,$$

where $a = (8\pi^2 c\mu\omega_e x_e/h)^{1/2} = 0.2454(\mu\omega_e x_e)^{1/2}\,\mathrm{cm}^{-1}$, is the bond energy,

$$D_e = \omega_e^2/4\omega_e x_e, \qquad (1)$$

r_e is the equilibrium bond length (Å), and μ is the reduced mass (in carbon units). All these quantities can be determined experimentally. If the bond energy D_e is unknown, the approximation $M1(r)$ is used, in which its expected value D'_e is determined from equation (1) using ω_e and $\omega_e x_e$ obtained from the first two vibrational transitions 0−1 and 1−2. If D_e is known, approximation $M2(r)$ can be used, where the constant $\omega_e x'_e$ is determined from equation (1) using D_e and ω_e. Hereafter, the prime denotes an approximation parameter defined by equation (1), which plays an important role in the subsequent exposition.

It should be noted that the precursor to Morse's approach [6] can be considered the empirical Borg-Sponer extrapolation — a graphical estimate of the dissociation energy of a diatomic molecule in the coordinates $E(\nu)$ and $(\nu + 1/2)$ [7,8]. These reviews present extensive experimental data illustrating attempts to systematize vibrational structures of electronic spectra without using the then unintroduced concept of anharmonicity.

2. Simple term

An example of a simple term is the ground state $X^1\Sigma_g^+$ of the F_2 molecule (Fig. 1), described in [5]. A hallmark of simple terms is that the real curve lies between $M1(r)$ (upper curve) and and $M2(r)$ (lower curve) without crossings. Figure 2 shows the differences $\delta(r) = U(r) - M1(r)$ and $\delta(r) = U(r) - M2(r)$ for this

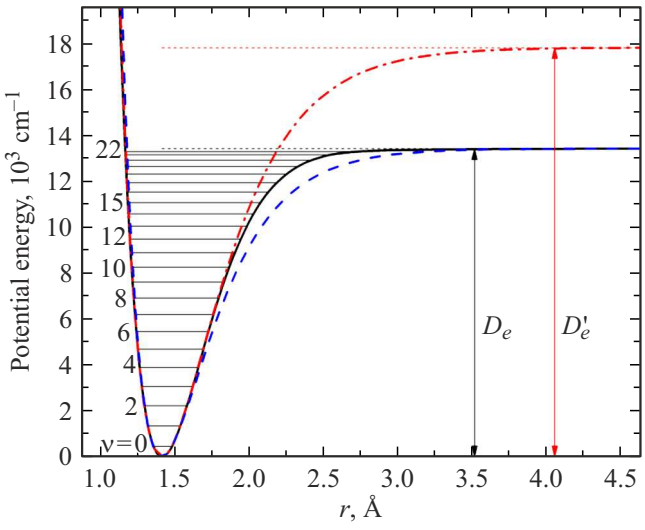

Figure 1. The ground state term $X^1\Sigma_g^+$ of the F_2 molecule (black solid curve) and its approximations $M1(r)$ (red dash-dotted curve) and $M2(r)$ (blue dashed curve), constructed from literature data [5].

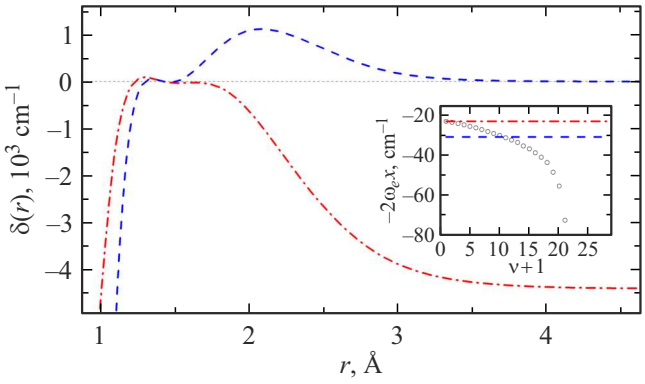

Figure 2. Differences $\delta(r)_{M1} = U(r) - M1(r)$ (red dash-dotted curve) and $\delta(r)_{M2} = U(r) - M2(r)$ (blue dashed curve) for the ground state term $X^1\Sigma_g^+$ of the F_2 molecule. Inset: experimental values of the anharmonicity function $-2\omega_e x(v)$ and its constant values for $M1(r)$ (red dash-dotted line) and $M2(r)$ (blue dashed line).

term, quantitatively demonstrating its approximation results. For a simple term at $r > r_e$ for $M1(r)$ $\delta(r) < 0$ and for $M2(r)$ $\delta(r) > 0$ hold.

In the inset of Fig. 2 for this term, values of the empirical anharmonicity function $-2\omega_e x(v)$ introduced in [5] as $\Delta_2 G(v)$ are given. Its monotonic increase in absolute value at higher vibrational excitation levels is a characteristic feature of a simple term. For the $M1(r)$ and $M2(r)$ approximations, the constant value of this function is determined by the constants $2\omega_e x_e$ and $2\omega_e x'_e$ respectively. The constant $\omega_e x'_e$ could, like $\omega_e x_e$ become an important spectroscopic constant of diatomic molecules [9,10].

3. Inversion of anharmonicity

For the terms of some molecules, the bond energy D'_e obtained in the $M1(r)$ approximation and calculated by equation (1) is less than the actual bond energy D_e of the real term $U(r)$. For simple terms $D'_e > D_e$ and the width of $M1(r)$ is smaller than those of $U(r)$ and $M2(r)$. Therefore, for simple terms $\omega_e x_e < \omega_e x'_e$. However, in Table 1 of Morse's work [6], several examples are given where $D'_e < D_e$. Terms meeting the condition $\Delta\omega_e x_e \equiv \omega_e x_e - \omega_e x'_e > 0$ will be called terms with inversion of anharmonicity. Such inversion occurs in complex terms whose lower part is broadened compared to simple terms, causing an increase in the density of vibrational levels (Tables 1 and 2 of [11]). The distinct feature of anharmonicity inversion is that it affects only terms $M1$, whereas terms $M2$ retain their form. Under inversion, for $r > r_e$ the $M1(r)$ curve extends beyond the potential well of $U(r)$, possible crossings with $U(r)$ occur, and the difference $\delta(r)_{M1}$ becomes positive over at least part of the internuclear distance range.

A typical example of terms with anharmonicity inversion is the potential curves of the ground state $X^2\Sigma_g^+$ of hydrogen ion cations H_2^+ and its isotopologues. Figure 3 plotted based on [12], shows the term D_2^+ and its approximation by $M1(r)$ and $M2(r)$ functions. The $M1(r)$ curve lies below $M2(r)$ throughout the potential well due to anharmonicity inversion, and the distance between them increases monotonically, resulting in the asymptote D'_e being $\sim 1800\,\text{cm}^{-1}$ lower than the bond energy D_e. The $M2(r)$ curve closely follows $U(r)$ initially inside the well and then crossing $U(r)$ at $r \sim 3.3$ Å outside the well (around 85% of its depth). This crossing is better tracked on the plot of the difference $\delta(r)_{M2}$ (Fig. 4). The shape of the $M2(r)$ curve in the lower part of the term is influenced by a large Herzberg anomaly [1], forming a dome-shaped minimum on the $\delta(r)_{M2}$ difference curve. This reveals a large anharmonicity value $\omega_e x_e$ caused by a significant expansion of the D_2^+ potential near the well bottom. The normal course of the $M2(r)$ curve below $U(r)$ is restored after the crossing at $r \sim 3.3$ Å shown as a small maximum on the $\delta(r)_{M2}$ curve at $r \sim 4$ Å (Fig. 4.).

The concept of the „Herzberg anomaly" was introduced in [1] and later mentioned in [2,4] during analysis of the hydrogen molecule H_2 ground term and distortions manifested in the shape of the function $M2(r)$. This anomaly, consisting of a broadening of the $U(r)$ function contour in the lower part of the attraction branch, was shown in Herzberg's book [13] (Fig. 48) and for a long time remained the only indication of distortions accompanying the approximation. It was subsequently found that such an anomaly commonly occurs in diatomic molecules and sometimes reaches significant magnitude.

For the $M1(r)$ function, the difference $\delta(r)_{M1}$ is also influenced by the Herzberg anomaly. According to [2,4], the presence of the Herzberg anomaly at the ground term

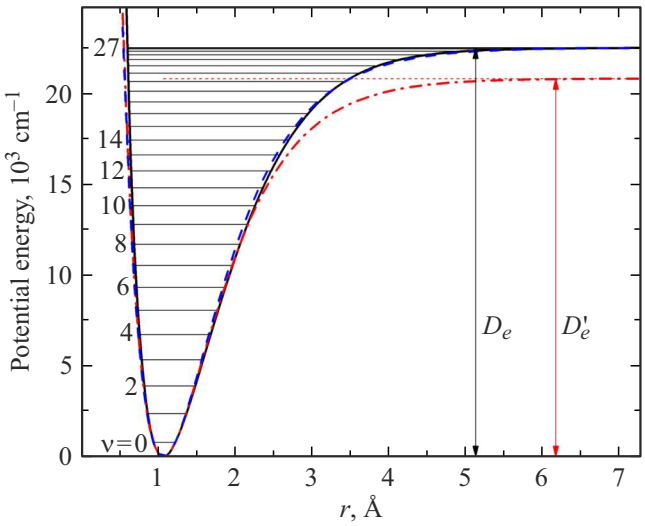

Figure 3. Ground state term $X^2\Sigma_g^+$ of the D_2^+ cation [12] and its approximations by $M1(r)$ ($D'_e = 20832.7\,\text{cm}^{-1}$, $\omega_e = 1641.62\,\text{cm}^{-1}$, $\omega_e x_e = 32.34\,\text{cm}^{-1}$ red dash-dotted curve) and $M2(r)$ ($D_e = 22525.7\,\text{cm}^{-1}$, $\omega_e = 1641.62\,\text{cm}^{-1}$, $\omega_e x'_e = 29.91\,\text{cm}^{-1}$ blue dashed curve).

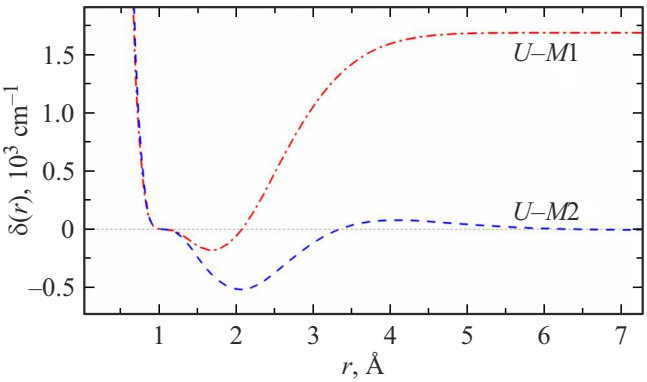

Figure 4. Differences $\delta(r)_{M1} = U(r) - M1(r)$ (red dash-dotted curve) and $\delta(r)_{M2} = U(r) - M2(r)$ (blue dashed curve) for the ground state term $X^2\Sigma_g^+$ of the D_2^+ cation according to [12].

H_2 potential curve and its isotopologues leads to a loss of monotonicity and appearance of extrema in the difference curve, allowing crossings with $U(r)$. For example, the region with a minimum at $r \sim 1.7$ Å before a crossing at $r \sim 2$ Å is caused by the predominance of the Herzberg anomaly, similar to the H_2 term.

Additional details on the potential curve with anharmonicity inversion can be gained from analyzing the vibrational structure $G(v)$ of the $U(r)$ term using the curves of first and second differences (Fig. 5):

$$\Delta_1 G(v) = G(v+1) - G(v),$$

$$\Delta_2 G(v) = G_1(v+1) - G_1(v).$$

The anharmonicity function $\Delta_2 G(v)$ demonstrates convergence of vibrational levels as dissociation asymptote is approached. This function was previously employed to describe vibrational structures of cation complexes with inert gases in Borg-Sponer coordinates [11,14,15]. The red dash-dotted and blue dashed lines characterize the appearance of functions $M1(v)$ and $M2(v)$ respectively. Their slopes are determined by anharmonicities $\omega_e x_e$ and $\omega_e x'_e$. Experimental points lie close to the $M2(v)$ line, indicating that the real $U(r)$ function is adequately described by this Morse function. The extrapolated maximum vibrational quantum number for $M2(v)$ corresponds to its actual value $v_{\max} = 27$, as expected since the construction of $M2$ uses the real value D_e. As a result of anharmonicity inversion, it lies above the $M1$ line, with a shallower slope against the abscissa axis.

The vibrational structure of the $U(r)$ term is more precisely and clearly demonstrated by the anharmonicity function $\Delta_2 G(v)$ shown as hollow points in Fig. 5. Over a wide segment of the potential well, the magnitude of this function decreases (a sign of the Herzberg anomaly [1,4]), passes through a maximum at $v \sim 11$ and then increases monotonically. Near the asymptote, there is an abrupt decrease in the anharmonicity magnitude from 73 ($v = 23$) to 43 cm^{-1} ($v = 25$). This jump was found by the authors [1] when analyzing the $\Delta_2 G(v)$ sequence in the ground term of Li_2 and O_2 molecules and is presumably explained by a change in the type of interatomic bond at the outer turning point for large-amplitude vibrations. The basis for this was the observation made in [1] of the monotonically increasing nature of the function $\Delta_2 G(v)$ for van der Waals molecules ArXe, Kr_2 and Xe_2. A similar jump was also noted for the ground terms of B_2, TF, Na_2, Cs_2, ICl, N_2, LiFr. The question of its origin remains open and requires theoretical analysis. The dashed lines parallel to the abscissa axis indicate that as a result of inversion, the anharmonicity $M1(v)$ (red) increased and became larger than $M2(r)$ (blue).

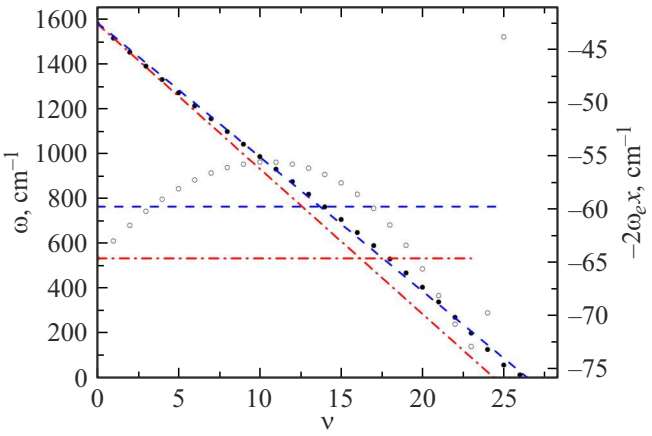

Figure 5. Functions $\Delta_1 G(v)$ (•) and $\Delta_2 G(v)$ (○) for the ground state term $X^2\Sigma_g^+$ of the D_2^+ cation and their appearances in $M1(r)$ (red dash-dotted lines) and $M2(r)$ (blue dashed lines) approximations.

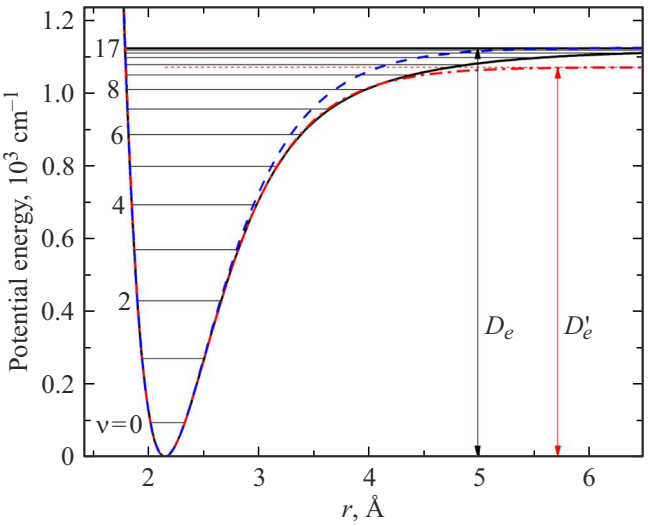

Figure 6. Ground state term $X^2\Pi_{1/2}$ of the C^+-Ne complex, built data [14], and its approximations by $M1(r)$ ($D'_e = 1069\,\text{cm}^{-1}$, $\omega_e x_e = 8.70\,\text{cm}^{-1}$ red dash-dotted curve) and $M2(r)$ ($D_e = 1122.7\,\text{cm}^{-1}$, $\omega_e x'_e = 8.29\,\text{cm}^{-1}$ blue dashed curve).

The inversion of anharmonicity is well illustrated by the potential curve of the ground state $X^2\Pi_{1/2}$ of the C^+-Ne complex and its approximations $M1(r)$ and $M2(r)$ (Fig. 6). The extrapolated bond energy D'_e is $53\,\text{cm}^{-1}$ less than the actual value D_e. The $M1(r)$ curve lies significantly below $M2(r)$ throughout the potential well but closely follows $U(r)$ only departing to the asymptote at D'_e after crossing $U(r)$ at 4 AA.

The differences $\delta(r)$ for the C^+-Ne complex demonstrate complex behavior (Fig. 7). The $M1(r)$ curve initially lies outside the potential well but from $r \sim 3$ Å to the crossing at 4 Å remains inside, signaling broadening of the $U(r)$ term. Above 4 Å anharmonicity inversion dominates and the difference $\delta(r)_{M1}$ monotonically approaches its limit. The $M2(r)$ function is not affected by anharmonicity inversion and lies within the real term, $\delta(r)_{M2} < 0$ indicating the presence of an anomaly in the $U(r)$ function, characterized by broadening of the $U(r)$ contour over a large interval up to the asymptote. This type of anomaly, hereafter called Anomaly2, was described in [16], shown in Fig. 3 at the ground term of Be_2. Using the example of the Be_2 ground term, distortion of the Morse approximation potential shape was shown, where the $M2(r)$ curve initially lies outside $U(r)$ and after crossing falls inside the potential well. The authors attributed this to a change in interatomic bonding type from valence to van der Waals. A more detailed discussion of the Be_2 term was given earlier [1,4].

In the search for spectral manifestations of increasing valence bonding features in the series C^+-RG (RG = He–Xe) the authors of [14] performed graphical analysis of the vibrational structure of electronic terms of the ground $^2\Pi_{1/2}$ and excited $^2\Sigma^+_{1/2}$ states of the complexes using $\Delta_1 G(v)$ dependencies (Birge-Sponer diagrams). For these dependencies, a line drawn through the first two points (Birge-Sponer line) allows determination of spectral constants ω_e, $\omega_e x_e$ and the bond energy D'_e [17] and sets the parameters of the $M1$ model. The family of experimental or theoretical vibrational frequency values of the real $U(r)$ term in these coordinates is its individual characteristic and in particular allows to determine parameters of $M2$ for the known value of D_e given the known value D_e. The authors noted that in the ground state, the central part of the diagram for Ar–Xe complexes has a steeper slope than the Borg-Schponer line, unlike lighter He and Ne atoms. Calculation of electronic structure of complexes in this series by several methods showed increasing charge transfer to the cation, negligible for C^+ complexes with He and Ne but for subsequent members it was interpreted as small chemical interaction. This agrees with vibrational frequency analysis via Birge-Sponer and is confirmed by data for the excited electronic state $^2\Sigma^+_{1/2}$ of these complexes. In the excited state, charge transfer is increased, and all complexes in the series show a steep slope in $\Delta_1 G(v)$ dependence.

Analysis of the potential curves and $\Delta_1 G(v)$ differences of the $^2\Sigma^+_{1/2}$ term of the C^+-Kr complex shows the development of anharmonicity inversion manifestations with increasing valency in the C^+-RG series. Figure 8 shows difference curves $\delta(r)$ for this term, constructed using data from [14]. For this term, $\omega_e x_e = 3.86\,\text{cm}^{-1}$ and $\omega_e x'_e = 3.25\,\text{cm}^{-1}$, while the extrapolated dissociation energy $D'_e = 1333\,\text{cm}^{-1}$ is $\sim 230\,\text{cm}^{-1}$ less than the true value $1562.8\,\text{cm}^{-1}$. For this term, the $M2(r)$ curve lies entirely outside the $U(r)$ function, and Anomaly2 occupies the entire potential well. Its shape resembles the $M2(r)$ function of a simple term, i.e., $M2(r)$ and $U(r)$ are close. The difference $\delta(r)_{M1}$ shows this function does not undergo significant influence from Anomaly2. Anharmonicity inversion influence appears starting from the lower part of the potential well.

It should be noted that literature data are not limited to the examples above. Systematic studies of bonding nature

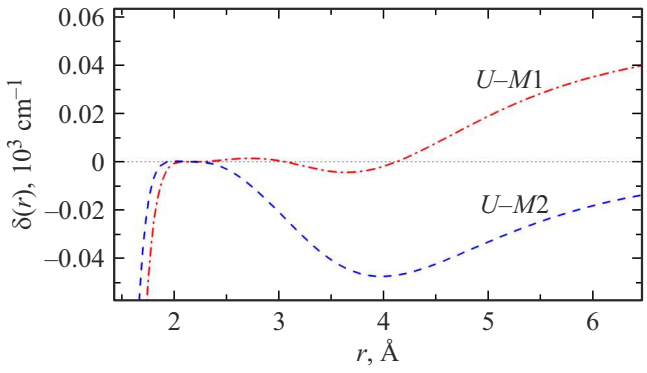

Figure 7. The differences $\delta(r)_{M1} = U(r) - M1(r)$ (red dash-dotted curve) and $\delta(r)_{M2} = U(r) - M2(r)$ (blue dashed curve) for the ground state term $X^2\Pi_{1/2}$ of the C^+-Ne complex according to the data provided in [14].

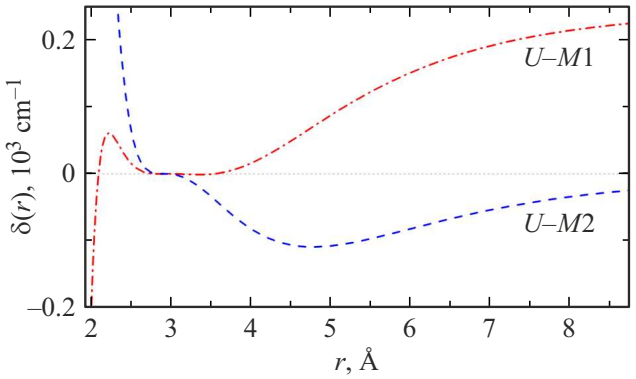

Figure 8. Differences $\delta(r)_{M1} = U(r) - M1(r)$ (red dash-dotted curve) and $\delta(r)_{M2} = U(r) - M2(r)$ (blue dashed curve) for the $^2\Sigma^+_{1/2}$ term of the C^+-Kr complex [14].

and spectral characteristics of M^+-RG ($M = C, Si, Ge$; $RG = He-Xe$) [11,14,15,18] complexes have been performed. Potential curves and vibrational frequencies were obtained for several dozen complexes; Birge-Sponer dependencies (the $\Delta_1 G(v)$ function in our terminology) were studied, and bond energy estimates were derived. These results are important for understanding the prospects of applying Morse-analysis of potential functions. They show significant diversity in appearance of vibrational structure of the set of similar complexes and validate the next step: studying the anharmonicity function $\Delta_2 G(v)$. Increasing precision of calculations opens opportunities to analyze potential curve contours near the dissociation asymptote, where van der Waals interactions may make a significant contribution. Accumulation of data and interpretation are needed regarding the sharp decrease in anharmonicity near the asymptote, observed in vibrational spectra analysis of several molecules, including van der Waals types. Finally, analysis of $M1(r)$ and $M2(r)$ curves could lead to qualitatively new insights on terms with anharmonicity inversion.

4. Conclusion

The features of approximating an electronic term of a diatomic molecule $U(r)$ by the Morse formula, a simplest, single-parameter anharmonic potential, admitting two possible solutions were discussed. The $M1(r)$ function is constructed using the experimental anharmonicity $\omega_e x_e$ of $U(r)$ determined from vibrational transitions $0-1$ and $0-2$, and extrapolates the bond energy D'_e, which usually exceeds the true value D_e due to vibrational level crowding near the potential well's middle. The $M1(r)$ function describes the lower half of the $U(r)$ curve well; their divergence increases monotonously approaching the dissociation asymptote. The $M2(r)$ model is built using the known D_e, with anharmonicity parameter x'_e defined as $x'_e = \omega_e / 4D'_e$. It describes the upper part of the $U(r)$ term well, but provides slightly worse description of the lower part, then $M1(r)$. The divergency shows a dome-like shape with a maximum near two-thirds depth of the potential well.

Increase of the parameter x'_e leads to a new spectral property — anharmonicity inversion, characteristic for complex terms where lower part of potential is broadened by peculiar interatomic interactions, increasing the density of lower vibrational levels. Anharmonicity inversion affects the behavior of the $M1(r)$ term: its extrapolated bond energy D'_e becomes less than the true value D_e.

It is shown that distinctive features of the experimental $U(r)$ term are clearly reflected in the graph of the anharmonicity function $\Delta_2 G(v)$.

Acknowledgments

The authors would like to thank Prof. V.P. Bulychev, I.G. Denisov, and I.G. Shenderovich for their continued interest, detailed and critical discussions, and valuable advices.

Conflict of interest

The authors declare that they have no conflict of interest.

References

[1] G.S. Denisov, I.G. Denisov. Spectr. Acta A, **262**, 120111 (2021). DOI: 10.1016/j.saa.2021.120111
[2] G.S. Denisov, E.R. Chakalov, P.M. Tolstoy. Spectr. Acta A, **327**, 125410 (2025). DOI: 10.1016/j.saa.2024.125410
[3] G.S. Denisov, K.G. Tokhadze. Opt. Spectrosc., **130** (14), 2096 (2022). DOI: 10.21883/EOS.2022.14.53993.2483-21
[4] G.S. Denisov. Opt. Spectrosc., **130** (9), 1058 (2022). DOI: 10.21883/EOS.2022.09.54819.3590-22
[5] G.S. Denisov, R.E. Asfin. Spectrosc. Lett., **57** (10), 553 (2024). DOI:10.1080/00387010.2024.2385627
[6] P.M. Morse. Phys. Rev., **34** (1), 57 (1929). DOI: 10.1103/PhysRev.34.57
[7] A.G. Gaydon. Proc. Phys. Soc., **58** (5), 525 (1946). DOI: 10.1088/0959-5309/58/5/302
[8] A.G. Gaydon. *Dissociation Energies and Spectra of Diatomic Molecules*, 3rd ed. (Chapman & Hall, London, 1968).
[9] *Spectral Constants of Diatomic Molecules* section 9. In: *CRC Handbook ofChemistry and Physics*, 103rd ed. (CRC Press: Boca Raton, FL, 2022).
[10] K.P. Huber, G. Herzberg. *Molecular Spectra and Molecular Structure. IV. Constants of Diatomic Molecules* (Springer, US: Boston, MA, 1979). DOI: 10.1007/978-1-4757-0961-2_2
[11] W.D. Tuttle, J.P. Harris, V. Jeong, W.H. Breckenridge, T.G. Wright. J. Phys. Chem. A, **122** (38), 7679 (2018). DOI: 10.121/acs.jpca8b07139
[12] C. Fábri, G. Czakó, G. Tasi, A.G. Császár. J. Chem. Phys., **130** (13), 134314 (2009). DOI: 10.1063/1.3097327
[13] G. Herzberg. *Molecular Spectra and Molecular Structure. I. Spectra of Diatomic Molecules* (D. Van Nostrand Company, New York, 1939).
[14] W.D. Tuttle, R.L. Thorington, L.A. Viehland, W.H. Breckenridge, T.G. Wright. Phil. Trans. R. Soc. A, **376** (2115), 20170156 (2018). DOI: 10.1098/rsta.2017.0156

[15] A.R. Davies, A. Cranney, L.A. Viehland, T.G. Wright. Phys. Chem. Chem. Phys., **24** (11), 7144 (2022). DOI: 10.1039/d1cp05710c
[16] J.M. Merritt, V.E. Bondybey, M.C. Heaven. Science, **324** (5934), 1548 (2009). DOI: 10.1126/science.1174326
[17] L. Lessinger. J. Chem. Educ., **71** (5), 388 (1994). DOI: 10.1021/ed071p388
[18] W.D. Tuttle, R.L. Thorington, L.A. Viehland, T.G. Wright. Molec. Phys., **113** (23), 3767 (2015). DOI: 10/1080/00268976.2015.106115

Translated by J.Savelyeva